

## ARTICLES

## Characterization and HDS Activity of Cobalt Molybdenum Nitrides

Kenichiro Hada, Masatoshi Nagai,\* and Shinzo Omi

*Graduate School of Bio-Applications and Systems Engineering, Tokyo University of Agriculture and Technology, 2-24 Nakamachi, Koganei, Tokyo 184-8588, Japan**Received: June 13, 2000; In Final Form: March 1, 2001*

The characterization of cobalt molybdenum nitrides with various cobalt contents has been studied using XRD, TEM, XPS, and temperature-programmed reactions with  $\text{NH}_3$ . The hydrodesulfurization of thiophene on the cobalt molybdenum nitride was carried out using a differential microreactor at atmospheric pressure. The XRD analysis of Co(50)973 indicated that  $\text{Co}_3\text{Mo}_3\text{N}$  was formed from the nitriding of a  $\text{CoMoO}_4$  precursor prepared from  $\text{Co}(\text{NO}_3)_2 \cdot 6\text{H}_2\text{O}$  and  $(\text{NH}_4)_6\text{Mo}_7\text{O}_{24} \cdot 4\text{H}_2\text{O}$  but not from the mixture of  $\text{CoO}$  and  $\text{MoO}_3$ . Co(10–25)973 had a high surface area of 120–129  $\text{m}^2 \text{g}^{-1}$ , but Co(50)973 had that of 12  $\text{m}^2 \text{g}^{-1}$ . The BET surface area was related to the molybdenum ions ( $\text{Mo}^{2+}$  and  $\text{Mo}^{3+}$ ) and cobalt ion ( $\text{Co}^{3+}$ ) in the bulk sample. The XPS and elemental analyses of Co(50)973 showed that the bulk composition was  $\text{Co}_3\text{Mo}_3\text{N} \cdot \text{N}_{0.2}$  and the surface composition was  $\text{Co}_3\text{Mo}_3\text{N} \cdot \text{N}_2$ . The cobalt molybdenum nitride Co(0–35)973 was more active than cobalt molybdenum sulfide on basis of catalyst weight in the hydrodesulfurization of thiophene at 623 K.

## Introduction

Transition-metal nitrides are active during hydrodesulfurization (HDS)<sup>1–12</sup> and hydrodenitrogenation<sup>2,8,13–21</sup> and are reported to have a turnover frequency higher than commercial Co–Mo<sup>8,15</sup> and Ni–Mo<sup>20</sup> sulfide catalysts on the basis of the CO and  $\text{O}_2$  adsorption. Recently, novel bimetallic nitrides and oxynitrides such as Co–Mo,<sup>22–30</sup> Fe–Mo,<sup>25,31</sup> Ni–Mo,<sup>31,32</sup> and V–Mo<sup>23,24,33</sup> were studied with respect to the catalytic activity and properties of the samples when synthesizing by temperature-programmed nitriding of the bimetallic oxides and a mixture of the monometallic oxides. Bem et al.<sup>31</sup> reported the synthesis of  $\text{Ni}_3\text{Mo}_3\text{N}$  by nitriding  $\text{NiMoO}_4$  at 973 K with ammonia and  $\text{Fe}_3\text{Mo}_3\text{N}$  by nitriding  $\text{FeMoO}_4$  at 1073 K. Also,  $\text{Co}_3\text{Mo}_3\text{N}$  was prepared from temperature-programmed nitriding of the  $\text{CoMoO}_4$  precursor at a final temperature of 973 K<sup>22,25–29</sup> and of  $\text{NH}_5(\text{CoOHMoO}_4)$  via Co metal and  $\gamma\text{-Mo}_2\text{N}$  intermediates at about 880 K.<sup>30</sup> On the other hand, Oyama et al.<sup>23,24</sup> reported Co–Mo oxynitrides during nitriding of a physical mixture of cobalt and molybdenum oxides via a solid-state reaction. Although the formation of cobalt molybdenum nitride from an oxidic precursor has been the subject of study for a long time, there is little agreement as to the precursor of cobalt molybdenum nitride. Furthermore, only a few attempts have so far been made to determine the oxidation states of the cobalt and molybdenum species in the nitrides. For the surface area of the nitrides, the Co–Mo oxynitride had a high surface area (103  $\text{m}^2 \text{g}^{-1}$ )<sup>23,24</sup> on one side and  $\text{Co}_3\text{Mo}_3\text{N}$  had a low surface area (19  $\text{m}^2 \text{g}^{-1}$ )<sup>22</sup> on the other. Although a large number of studies have been carried out on the high surface area, little is known about the relation between the high surface area and the composition of the cobalt molybdenum nitrides. Moreover, no

attention has been paid to whether bimetallic nitrides had high surface areas and the composition on the surface and in the bulk of the cobalt molybdenum nitrides. Although the preparation and characterization of passivated bimetallic nitrides were extensively studied ex situ on the basis of XRD,<sup>22–24,31–33</sup> there have been few studies on the in situ characterization of the nitrides using XPS with a complement to XRD. The XPS analysis can provide the oxidation states and compositions of metal atoms in the bulk and on the surface of the samples. More recently, the catalytic activities of supported and unsupported Co–Mo nitrides for hydroprocessing over bimetallic nitrides were studied.<sup>6,22,27,29</sup> Kim et al.<sup>22</sup> and Bussell and co-workers<sup>27</sup> reported that cobalt molybdenum nitrides had greater HDS activity than  $\gamma\text{-Mo}_2\text{N}$ . In this study, the cobalt molybdenum nitrides are synthesized at a temperature of 973 K via nitriding of the precursor prepared from  $\text{Co}(\text{NO}_3)_2 \cdot 6\text{H}_2\text{O}$  and  $(\text{NH}_4)_6\text{Mo}_7\text{O}_{24} \cdot 4\text{H}_2\text{O}$  and from a mixture of  $\text{CoO}$  and  $\text{MoO}_3$ . Also, the formation and composition of cobalt molybdenum nitride in the bulk sample and on the surface are confirmed by XRD and XPS along with changing the ratio of Co/(Co + Mo) in the cobalt molybdenum oxides. The relationship between the surface area and the cobalt and molybdenum species of the samples are analyzed on the basis of the XPS spectra of Co 2p, Mo 3d, and N 1s of the samples. The catalytic activities of the cobalt molybdenum nitride samples were tested in thiophene HDS reactions at 623 K and atmospheric pressure.

## Experimental Section

**Preparation of Cobalt Molybdenum Nitride.** Oxidic precursors with several Co/(Co + Mo) ratios were prepared using a mixture of an aqueous solution of cobalt nitrate ( $\text{Co}(\text{NO}_3)_2 \cdot \text{H}_2\text{O}$ ) (Kishida Chemical Co., 99%) and ammonium heptamolybdate  $(\text{NH}_4)_6\text{Mo}_7\text{O}_{24} \cdot 4\text{H}_2\text{O}$  (Kishida Chemical Co., 99%). The solid products were dried at 373 K overnight and calcined

\* To whom correspondence should be addressed. Phone and fax: +81 (0)42 388 7060. E-mail: mnagai@cc.tuat.ac.jp.

at 773 K for 7 h in dry air. The precursors were placed on a fritted quartz plate in a 10 mm i.d. quartz microreactor and then nitrified by a temperature-programmed reaction (TPR) with ammonia (99.99%). A 0.2 g sample was oxidized in dry air (1.11 mL s<sup>-1</sup>) at 723 K for 1 h for an oxidized sample. For nitrified samples, the 0.2 g sample was oxidized in dry air at 723 K for 1 h, cooled from 723 to 573 K in dry air, nitrified from 573 to 973 K at a rate of 0.0167 K s<sup>-1</sup> with 1.11 mL s<sup>-1</sup> of ammonia, held at this temperature for 3 h, and then cooled to room temperature in flowing ammonia. The other oxidic precursor was prepared from a physical mixture of CoO and MoO<sub>3</sub> (Co/(Co + Mo)) = 0.5, after nitrifying the sample for comparison. To compare the catalytic properties of the nitrified catalysts with the sulfided catalyst, Co(25) was sulfided at 623 K under a stream of 10% H<sub>2</sub>S/H<sub>2</sub> (4 L h<sup>-1</sup>) after the catalyst was heated at 723 K in air. The sample names of the cobalt molybdenum samples are abbreviated Co(x)y, where  $x \times 10^{-2}$  is the atomic ratio of Co/(Co + Mo) in the oxides and nitrides and y is 723 K for oxidizing or is 773–1073 K for the nitrifying. For example, Co(20)723 denotes the cobalt molybdenum samples (Co(NO<sub>3</sub>)<sub>2</sub>·H<sub>2</sub>O and (NH<sub>4</sub>)<sub>6</sub>Mo<sub>7</sub>O<sub>24</sub>·4H<sub>2</sub>O with Co/(Co + Mo) = 0.2) oxidized at 723 K. Co(50)973 and Co(5–25)-973 denote the cobalt molybdenum samples with Co/(Co + Mo) = 0.5 and 0.05–0.25, respectively, nitrified with ammonia at 973 K.

**BET Surface Area.** The specific surface areas of the samples were measured using an Omnisorp 100CX (Beckman Coulter Co.). The surface area of the samples (0.1 g) was measured by nitrogen adsorption at liquid-nitrogen temperature after the sample was evacuated at 473 K and  $1.3 \times 10^{-4}$  Pa for 2 h.

**XRD.** The sample before and after nitrifying was measured by XRD. The nitrified sample was passivated in 1% O<sub>2</sub>/He (0.167 mL s<sup>-1</sup>) for longer than 12 h at room temperature after nitrifying. The diffraction pattern was obtained using a RAD-II (Rigaku Co.) equipped with Cu K $\alpha$  radiation ( $\lambda = 1.542$  Å). The peaks were identified on the basis of the JCPDS card references: MoO<sub>3</sub> (JCPDS 5-0508,  $2\theta = 12.8, 25.7, \text{ and } 27.4^\circ$ ; this study,  $2\theta = 12.9, 25.8, \text{ and } 27.4^\circ$ ), MoO<sub>2</sub> (JCPDS 32-671,  $2\theta = 26.1, 36.9, \text{ and } 53.2^\circ$ ; this study,  $2\theta = 26.0, 36.9, \text{ and } 53.6^\circ$ ),  $\gamma$ -Mo<sub>2</sub>N (JCPDS 25-1366,  $2\theta = 37.4, 43.5, \text{ and } 63.2^\circ$ ; this study,  $2\theta = 37.3, 43.5, \text{ and } 63.0^\circ$ ), CoO (JCPDS 43-1004,  $2\theta = 36.5, 42.4, \text{ and } 61.6^\circ$ ; this study,  $2\theta = 36.7, 42.3, \text{ and } 61.4^\circ$ ), Co metal (JCPDS 15-806,  $2\theta = 44.8, 47.6, \text{ and } 76.0^\circ$ ; this study,  $2\theta = 44.8, 47.5, \text{ and } 75.9^\circ$ ), and CoMoO<sub>4</sub> (JCPDS 21-868 and 25-1434,  $2\theta = 14.2, 26.7, \text{ and } 28.5^\circ$ ; this study,  $2\theta = 14.2, 26.5, \text{ and } 28.5^\circ$ ). The peaks of cobalt molybdenum nitride were consistent with the data reported by Jackson et al.<sup>25</sup> and Kim et al.<sup>22</sup> such that Co<sub>3</sub>Mo<sub>3</sub>N had peaks at  $2\theta = 40.0, 42.6, 46.6 \text{ and } 72.8^\circ$ . The peaks of Co–Mo oxynitride were identified by comparison with the data reported by Oyama and co-workers<sup>23</sup> at the broad peaks of  $2\theta = 37.0, 43.0, \text{ and } 63.0^\circ$ .

**Temperature-Programmed Reaction with NH<sub>3</sub> (TPR).** The oxidic precursor after oxidizing at 723 K was heated from 573 to 973 K at a rate of 0.167 K s<sup>-1</sup> with 1.11 mL s<sup>-1</sup> of ammonia (99.99%). The desorbed gases were monitored using a Balzers Quadstar 422 quadrupole mass spectrometer. Ammonia and water in the desorbing gases during TPR were qualitatively analyzed at  $m/z$  15 and 18, respectively, because they overlapped at  $m/z$  17. Hydrogen and nitrogen were monitored at  $m/z$  2 and 28, respectively.

**TEM.** The morphology of the samples was determined using a JEM-2000F transmission electron microscope (JEOL Co.) operating at 200 kV equipped with an energy-dispersive X-ray spectrometer (EDS). The sample was crushed in an agate pestle

and mortar, dispersed in ethanol with an ultrasonic apparatus, placed on a copper microgrid, and transferred to the analysis chamber in the TEM.

**XPS and Elemental Analysis.** X-ray photoelectron spectroscopy was carried out using a Shimadzu ESCA 3200 photoelectron spectrometer with Mg K $\alpha$  radiation (1253.6 eV, 8 kV, 30 mA). The samples after nitrifying were removed from the microreactor and then transferred to a glovebag in which the atmosphere was exchanged with argon (99.9999%) five times and filled with argon gas. The samples were mounted on a holder with carbon tape in the glovebag without exposure to air. Argon etching was done for the analysis of the bulk samples at a pressure of  $8 \times 10^{-4}$  Pa for 1 min. The analysis was typically done at a pressure of  $5 \times 10^{-6}$  Pa and at a scan speed of 0.33 eV s<sup>-1</sup> with 0.05 eV (step)<sup>-1</sup>. The binding energy of C 1s (284.6 eV) was taken as a reference to correct the binding energy of the samples. The envelopes of the XPS binding energies of Mo 3d, Mo 3p, Co 2p, and N 1s were deconvoluted using Origin package software (Microcal Co.) after the analytical data were transferred from the Shimadzu ESCA 3200 to a PC data station. Since the binding energies of XPS Mo 3d<sub>3/2</sub> and 3d<sub>5/2</sub> and Co 2p<sub>3/2</sub> and 2p<sub>1/2</sub> had many peaks (Mo<sup>0</sup>, Mo<sup>2+</sup>, Mo<sup>3+</sup>, Mo<sup>4+</sup>, Mo<sup>5+</sup>, and Mo<sup>6+</sup> and Co<sup>0</sup>, Co<sup>2+</sup>, and Co<sup>3+</sup>), the binding energies and fwhms of Mo 3d and Co 2p were fixed and deconvoluted, except for those of Co<sup>0</sup> (–0.5 to 0.5 eV deviation from the binding energy of Co<sup>0</sup> at 777.6 eV). The spectra of XPS Mo 3d of the cobalt molybdenum nitrified samples were deconvoluted using an intensity ratio of 2/3 and a splitting of 3.2 eV and referenced to the data reported by Hercules et al.<sup>34</sup> and Hada et al.<sup>35</sup> Mo<sup>0</sup> (Mo 3d<sub>5/2</sub> binding energy,  $227.7 \pm 0.2$ ; fwhm,  $1.2 \pm 0.2$ ), Mo<sup>2+</sup> ( $228.4 \pm 0.1$ ;  $1.4 \pm 0.2$ ), Mo<sup>3+</sup> ( $229.2 \pm 0.1$ ;  $1.5 \pm 0.3$ ), Mo<sup>4+</sup> ( $230.1$ ;  $1.6 \pm 0.2$ ), Mo<sup>5+</sup> ( $231.6$ ;  $1.65 \pm 0.2$ ), and Mo<sup>6+</sup> ( $233.0$ ;  $1.7 \pm 0.2$ ). Since the Co 2p spectra were very broad and difficult to deconvolute for both Co 2p<sub>3/2</sub> and 2p<sub>1/2</sub> in the region of 775–805 eV, the peaks of Co<sup>0</sup>, Co<sup>2+</sup>, Co<sup>3+</sup>, and Co<sup>2+</sup> satellites were fitted for only the Co 2p<sub>3/2</sub> region for all the samples. The peak fittings of the XPS Co 2p<sub>3/2</sub> binding energies were referenced to the data of cobalt molybdenum sulfides obtained by Pawelec et al.,<sup>36</sup> of CuCo/Al<sub>2</sub>O<sub>3</sub> by Figueiredo et al.,<sup>37</sup> and of Co/Al<sub>2</sub>O<sub>3</sub> by Zsoldos et al.<sup>38</sup> The Co 2p<sub>3/2</sub> binding energies for the cobalt molybdenum nitrified samples were deconvoluted to Co<sup>0</sup> (BE,  $777.6 \pm 0.8$  eV; fwhm,  $1.3 \pm 0.1$  eV), Co<sup>2+</sup> ( $779.9 \pm 0.4$  eV; 4.2 eV), Co<sup>3+</sup> ( $781.6 \pm 0.3$  eV;  $4.7 \pm 0.1$  eV), and Co<sup>2+</sup> satellite ( $786.1 \pm 0.3$ ; 5.0 eV). The base line corrections made of the peak fitting of Co 2p<sub>3/2</sub> and Mo 3d were carried out with the Shirley method provided by the Shimadzu spectrometer manufacturer. Furthermore, the XPS N 1s binding energy of the samples at  $397 \pm 0.3$  eV (fwhm 2.0 eV) was used to calculate the nitrogen content in the samples on the basis of a new determination method<sup>39</sup> for the deconvolution of Mo 3p<sub>3/2</sub> and N 1s in the region of 390 and 410 eV. Elemental analysis of the samples was carried out using a Shimadzu CHN 123 elemental analyzer (oxygen burning method) after the samples were evacuated at 673 K and  $1.3 \times 10^{-4}$  Pa for 2 h.

**HDS of Thiophene.** The flow system for the HDS of thiophene is described elsewhere.<sup>40</sup> The system consisted of a single-pass, differential microreactor. The HDS of thiophene on the nitride and sulfide catalysts (ca. 0.2 g) were carried out at 623 K and atmospheric pressure. The reaction feed, consisting of 3.8 vol % thiophene in pure hydrogen, was introduced at a rate of 50 mL min<sup>-1</sup> into the reactor. Quantitative analysis was performed by injecting a sample from a sampling loop into the gas chromatograph to analyze the amount of thiophene (column

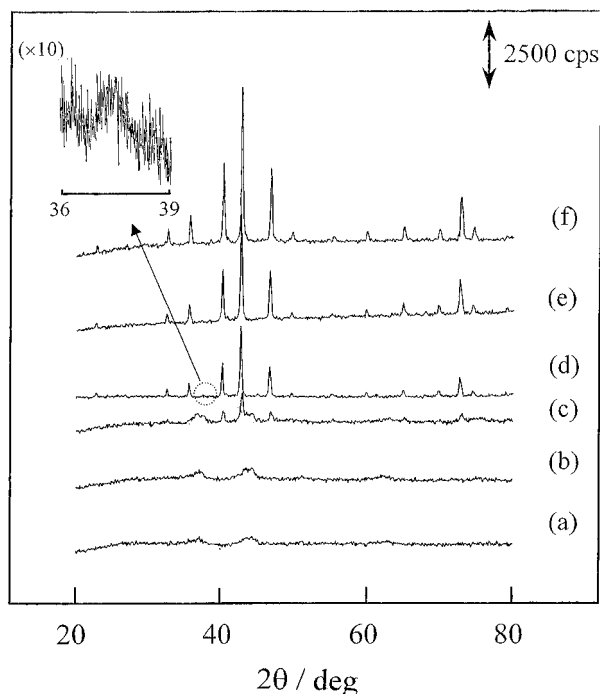


**Figure 1.** XRD patterns of cobalt molybdenum samples nitrided at various temperatures: (a) Co(50)773; (b) Co(50)873; (c) Co(50)923; (d) Co(50)973; (e) Co(50)1023; (f) Co(50)1073.

10% Silicon DC-550) at 348 K and reaction products (column VZ-8) at 313 K.

## Results and Discussion

**Formation of  $\text{Co}_3\text{Mo}_3\text{N}$ .** The XRD patterns of Co(50) nitrided at various temperatures are shown in Figure 1. The XRD measurement showed that  $\text{CoMoO}_4$  was observed in Co(50)-723 before nitriding. In Co(50)773–923 (Figure 1a–c), broad peaks were observed at around  $2\theta = 37$ , 43, and  $63^\circ$  and were probably characteristic of the formation of Co–Mo oxynitride.<sup>23</sup> The Co(50)923 sample (Figure 1c) was observed at new peaks of  $2\theta = 40.0$ , 42.6, 46.6, and  $72.8^\circ$  which were in agreement with  $2\theta = 40.0$ , 42.5, and  $46.5^\circ$  due to  $\text{Co}_3\text{Mo}_3\text{N}$  reported by Jackson et al.<sup>25</sup> and Kim et al.<sup>22</sup> The peak intensities increased with increasing nitriding temperature and sharpen with progressive increases in calcination temperature, indicating an increase in crystallinity of the cobalt molybdenum nitride. The patterns after nitriding at 1073 K are dominated by the characteristic patterns of  $\text{Co}_3\text{Mo}_3\text{N}$ . On the other hand, a very small peak was observed at about  $37.4^\circ$  in the XRD patterns of Co(50)973 (Figure 1d). This peak was different from that of Co–Mo oxynitride in the Co(50)773–923 samples but consistent with that of the  $\gamma\text{-Mo}_2\text{N}$  (111) phase. The amorphous  $\gamma\text{-Mo}_2\text{N}$  was slightly formed, together with  $\text{Co}_3\text{Mo}_3\text{N}$  in the Co(50)973 sample.

The profile of a temperature-programmed reaction (TPR) of the Co(50)723 sample, upon heating from 573 to 973 K at a rate of  $1 \text{ K min}^{-1}$  under a stream of excess  $\text{NH}_3$ , is shown in Figure 2. The formation peaks of  $\text{H}_2$  and  $\text{N}_2$  were observed above 780 K, while the formation peaks of  $\text{H}_2\text{O}$  were observed at about 750 and 900 K and the former peak of  $\text{H}_2\text{O}$  was larger than the latter peak. Below 820 K, ammonia decomposed and the hydrogen from ammonia was consumed for reduction of  $\text{CoMoO}_4$  to desorb  $\text{H}_2\text{O}$  and the nitrogen from ammonia-nitrided  $\text{CoMoO}_4$  to form Co–Mo oxynitride. Thus, the broad XRD patterns (in Figure 1a–c) showed the formation of Co–Mo

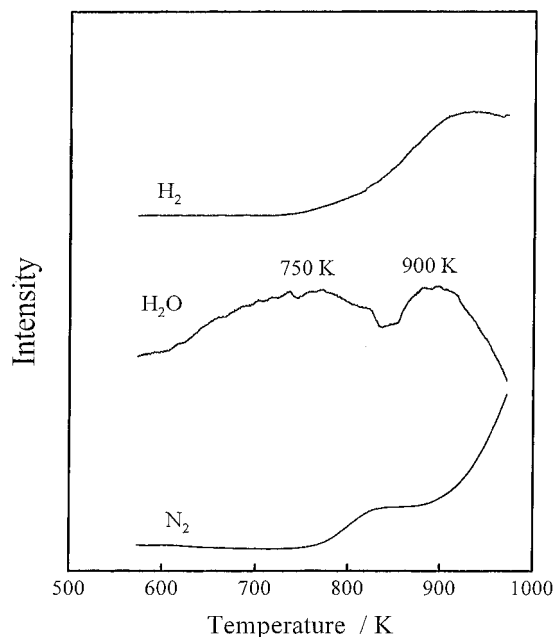
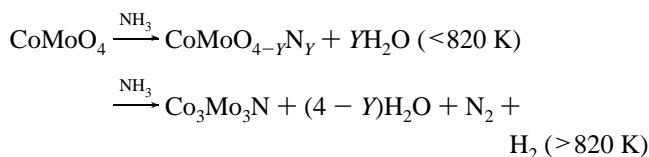


**Figure 2.** TPR profile of Co(50)723 under a stream of  $\text{NH}_3$ .

oxynitride in Co(50)773–Co(50)923. Moreover, a subsequent nitridation to Co–Mo oxynitride with  $\text{NH}_3$  started above 820 K to desorb  $\text{H}_2$  and  $\text{N}_2$ . The plateau of  $\text{N}_2$  formation at 820–880 K and the  $\text{H}_2\text{O}$  formation peak at 900 K were ascribed to the complete formation of  $\text{Co}_3\text{Mo}_3\text{N}$  from the nitriding of Co–Mo oxynitride. From the XRD results in Figure 1c, very broad peaks of Co–Mo oxynitride were observed for the Co(50)923 sample (the broad peaks at approximately  $37$ ,  $43$ , and  $63^\circ$ ), while cobalt molybdenum nitrides were observed for the Co(50)973 sample (Figure 1d). On the basis of the XRD and TPR data, we propose that the reaction of  $\text{CoMoO}_4$  with  $\text{NH}_3$  proceeds through the reaction pathway



Cobalt molybdenum samples nitrided at 973 K with various cobalt contents were analyzed using XRD before and after nitriding the mixture of cobalt nitrate and ammonium heptamolybdate at 973 K. The representative spectra are shown in Figure 3.  $\gamma\text{-Mo}_2\text{N}$  (Figure 3a) was formed, together with  $\text{MoO}_2$  for Co(5–25)973 (Figure 3b).  $\gamma\text{-Mo}_2\text{N}$  exhibited weak and broad peaks at  $2\theta = 37.4$ ,  $43.5$ , and  $63.2^\circ$ , which were close to the peaks of Co–Mo oxynitrides<sup>23</sup> ( $37.0$ ,  $43.0$ , and  $63.0^\circ$ ). Therefore, Co(25)973 contained  $\gamma\text{-Mo}_2\text{N}$  and probably amorphous and small particles of Co–Mo oxynitrides.  $\text{Co}_3\text{Mo}_3\text{N}$  had characteristic peaks of  $2\theta = 40.0$ ,  $42.7$ , and  $46.4^\circ$  for Co(50)-973 (Figure 3d). Since the Co(0–25)973 samples contained  $\gamma\text{-Mo}_2\text{N}$  and  $\text{MoO}_2$  which were contained in the Co(50)973 sample, the presence of a small amount of cobalt not only prevented the formation of  $\text{Co}_3\text{Mo}_3\text{N}$  but also prevented nitriding of the molybdenum oxides. For Co(35)973 and Co-(65)973, small amounts of  $\gamma\text{-Mo}_2\text{N}$  and Co metal were observed together with  $\text{Co}_3\text{Mo}_3\text{N}$ , respectively, as shown in Figure 3c,e. For the Co(90,100)973 samples, Co metal was only formed. On the other hand,  $\text{CoMoO}_4$  was only formed for Co(50)723 in Figure 3g and formed together with  $\text{MoO}_3$  for Co(10–35)-723 and with CoO for Co(65)723. From the results,  $\text{Co}_3\text{Mo}_3\text{N}$

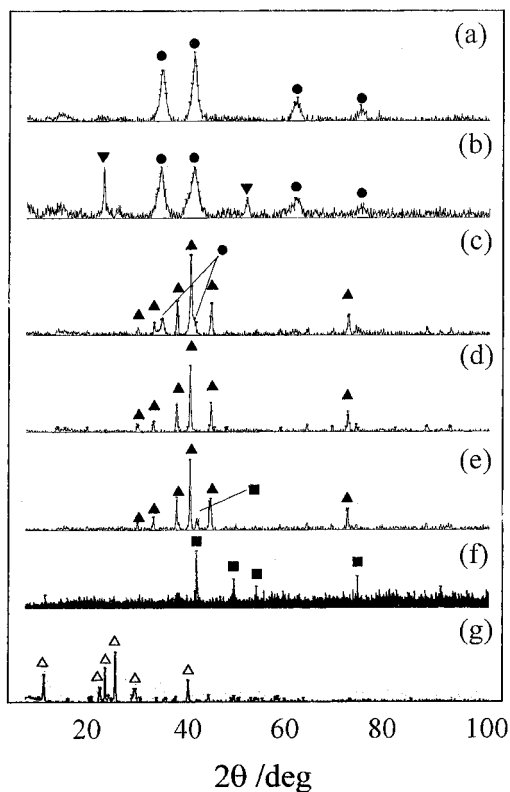


**Figure 3.** XRD patterns of cobalt–molybdenum nitrides and oxide with various Co loadings prepared from the mixture of cobalt nitrate and molybdenum heptamolybdate: (a) Co(0)973; (b) Co(25)973; (c) Co(35)973; (d) Co(50)973; (e) Co(65)973; (f) Co(100)973; (g) Co(50)973; (▼) MoO<sub>2</sub>; (●)  $\gamma$ -Mo<sub>2</sub>N; (▲) Co<sub>3</sub>Mo<sub>3</sub>N; (■) Co metal; (Δ) CoMoO<sub>4</sub>.

was formed from CoMoO<sub>4</sub> prepared from a mixture of cobalt nitrate and ammonium heptamolybdate. The cobalt molybdenum sample with Co/(Co + Mo) = 0.5 was analyzed using XRD before and after nitriding the physical mixture of CoO and MoO<sub>3</sub> at 973 K. Co<sub>3</sub>Mo<sub>3</sub>N did not have peaks of  $2\theta = 40.0, 42.7,$  and  $46.4^\circ$ , but  $\gamma$ -Mo<sub>2</sub>N and Co metal were observed in the XRD patterns (Figure 3a). Also, CoMoO<sub>4</sub> was not formed but CoO and MoO<sub>3</sub> were formed in the oxidic precursor (Figure 3b). CoMoO<sub>4</sub> was not formed by oxidizing the physical mixture of CoO and MoO<sub>3</sub> at 723 K. Co<sub>3</sub>Mo<sub>3</sub>N was not produced until CoMoO<sub>4</sub> was formed in the sample. Therefore, Co<sub>3</sub>Mo<sub>3</sub>N was not formed by nitriding the physical mixture of CoO and MoO<sub>3</sub> but was formed by nitriding CoMoO<sub>4</sub> in Co(35–65)973, which was prepared using the aqueous solution of the mixture of cobalt nitrate and ammonium heptamolybdate.

**Morphology of Co<sub>3</sub>Mo<sub>3</sub>N.** The TEM images of Co(50)973 and Co(0)973 are shown in Figure 4. Molybdenum and cobalt atoms were observed in the samples from the EDS analysis for Figure 4A, while only molybdenum atoms are observed for Figure 4B. From the image, the aggregation of large particles (a) was observed in all samples, while small particles (b) (ca. 5 nm) were partially agglomerated. The particles (a) (20–30 nm) were as large as Co<sub>3</sub>Mo<sub>3</sub>N particles at  $D_c = 36.3$  nm from the XRD results using Scherrer's equation for the peak of Co(50)973 at  $42.5^\circ$ . Since the Co/Mo atomic ratio of the particles (a) was about 1.0 from the EDS analysis, the particles (a) consisted of Co<sub>3</sub>Mo<sub>3</sub>N. On the other hand, despite the Co/Mo ratio of 0.3, the image of the particles (b) was similar to that of the particles (c) in Co(0)973 (a small peak of  $\gamma$ -Mo<sub>2</sub>N in Figure 1d). These results indicated that the small particles (b) consisted of  $\gamma$ -Mo<sub>2</sub>N with highly dispersed Co species. Thus, Co(50)973

did not consist of a single phase but contained the two phases  $\gamma$ -Mo<sub>2</sub>N and Co<sub>3</sub>Mo<sub>3</sub>N.

**High Surface Area.** The BET surface area of the cobalt molybdenum compounds nitrided at 973 K as a function of the Co/(Co + Mo) ratio is shown in Figure 5. The surface area of Co(0)973 was  $112 \text{ m}^2 \text{ g}^{-1}$ . The surface area of Co(10,25)973 increased to 123 and  $129 \text{ m}^2 \text{ g}^{-1}$ . The surface area of Co(50)973 was  $12 \text{ m}^2 \text{ g}^{-1}$ , but that of Co(100)973 was only  $4 \text{ m}^2 \text{ g}^{-1}$ . Thus, the addition of cobalt at 10–25% of the samples increased the high surface area but Co(50)973 had one-tenth the surface area of Co(10–25)973. The distributions of the mesopores and micropores in the samples are shown in Figure 6. The mesopores at 4–5 nm and micropores at 0.4–0.6 nm for Co(25)973 were larger than those for Co(0)973. Since the Co(0–25)973 samples contained  $\gamma$ -Mo<sub>2</sub>N from the XRD analysis and had micropores and mesopores with a high surface area, the addition of a small amount of cobalt to the molybdenum compounds increased the micropores of  $\gamma$ -Mo<sub>2</sub>N. For Co(35–65)973, the micropores at 0.4–0.6 nm disappeared, and therefore, the Co(35–65)973 samples had mesopores without micropores. Moreover, we found that the Co<sub>3</sub>Mo<sub>3</sub>N particles with a low crystallinity increased the surface area of  $\gamma$ -Mo<sub>2</sub>N.<sup>41</sup> The low-surface-area sample without micropores was probably due to the growth of the Co<sub>3</sub>Mo<sub>3</sub>N particle.

**Oxidation States and Compositions of Bulk by XPS.** The XPS binding energies of Mo 3d and Co 2p<sub>3/2</sub> for Co(0–100)973 were analyzed using XPS to determine the oxidation state and composition of cobalt molybdenum nitride. The representative spectra are shown in Figure 7. Co(0,50)973 had a large peak of Mo<sup>0</sup> centered at the binding energy of Mo 3d<sub>5/2</sub> of 227.7 eV. Co(5–25,90)973 had a large peak of Mo<sup>2+</sup> located at the binding energy of 228.4 eV, which was reported to be at 228.4<sup>25</sup> and 228.8 eV<sup>2</sup> for  $\gamma$ -Mo<sub>2</sub>N. The Co 2p<sub>3/2</sub> level of a zerovalent Co was observed at  $777.9 \pm 0.5 \text{ eV}$  ( $777.6 \pm 0.5 \text{ eV}$ <sup>37,38,42,43</sup>) for all the samples nitrided at 973 K. The distribution of molybdenum oxidation states in the Mo 3d spectra was calculated as the individual Mo peak area divided by the total Mo peak area, as shown in Figure 8A. Mo<sup>2+</sup> was distributed from 25 to 52% for all the catalysts, and Mo<sup>0</sup> was distributed at more than 30% for Co(20–90)973. The Mo<sup>3+</sup> and Mo<sup>4+</sup> ions were at 10–20% and Mo<sup>5+</sup> and Mo<sup>6+</sup> ions were present at less than 10%. Thus, the Co(35–65)973 sample with Co<sub>3</sub>Mo<sub>3</sub>N mainly consisted of Mo<sup>0</sup> and Mo<sup>2+</sup>. Furthermore, from the XRD and TEM analyses,  $\gamma$ -Mo<sub>2</sub>N was partially contained together with Co<sub>3</sub>Mo<sub>3</sub>N in Co(50)973, as mentioned before. Since the Co(50)973 sample included six types of Mo ions, these ions were probably due to the mixture of Co<sub>3</sub>Mo<sub>3</sub>N and  $\gamma$ -Mo<sub>2</sub>N in the samples. In Figure 8B, on the other hand, Co<sup>0</sup> increased for Co(5–25)973 and was relatively constant at 40% for Co(25–90)973. The distribution of Co<sup>2+</sup> ion was almost constant at 50%. The Co<sup>0</sup> and Co<sup>2+</sup> ions were distributed at 90% in the all samples. The amount of Co<sup>3+</sup> ion was much less than that of Co<sup>0</sup> and Co<sup>3+</sup>, except for Co(5–25)973. Thus, Mo<sup>0</sup>, Mo<sup>2+</sup>, Co<sup>0</sup>, and Co<sup>2+</sup> species were the most abundant species in the Co(35–65)973 samples.

The XPS binding energies of N 1s and Mo 3p for Co(0,25,50)973 are shown in Figure 9 and Table 1. One peak of N 1s and four peaks of Mo 3p<sub>3/2</sub> (Mo <sup>$\delta$</sup>  ( $\delta = 0-3$ ), Mo<sup>4+</sup>, Mo<sup>5+</sup>, and Mo<sup>6+</sup>) were deconvoluted in the range of 390–410 eV.<sup>39</sup> The binding energy of N 1s was observed at  $397.1 \pm 0.2 \text{ eV}$  (397.4 eV;<sup>39</sup> dissolved N) in Co(0–25)973 but shifted to 396.2 (396.3) eV in Co(35–65)973, at which the binding energy was close to 396.7 eV (Mo–N band<sup>39</sup>) or lower than those of the Mo–N bond (397.1, 397.4 eV<sup>44,45</sup>) and Co–N bond (398.1

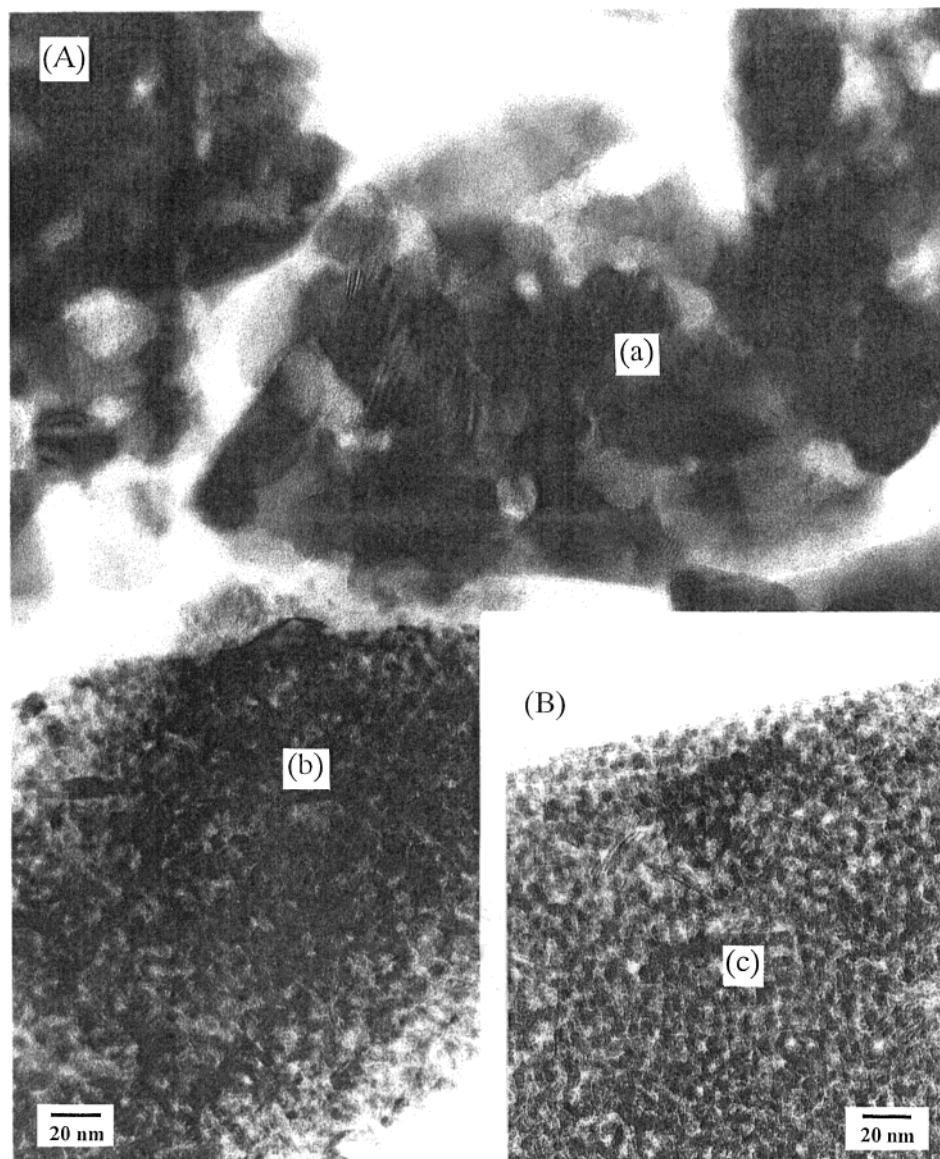


**Figure 4.** TEM images of the (A) Co(50)973 and (B) Co(0)973 samples.

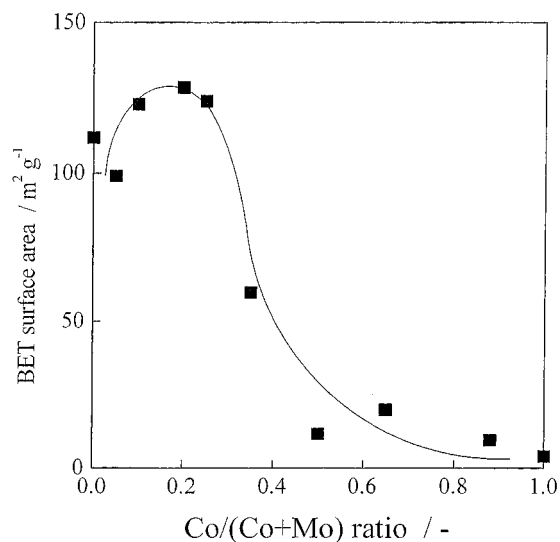


**Figure 5.** BET surface area as a function of Co/(Co + Mo) ratio for the 973 K nitrided cobalt–molybdenum.

eV<sup>46</sup>). The binding energy of the N 1s peak in the Co–Mo–N compounds was relatively close to the binding energy of N 1s

for the Mo–N bond, compared to that of the Co–N bond due to transferring electrons to the nitrogen atoms from cobalt. In Table 1, the ratios of N to Mo, calculated from the XPS data, were constant at 0.33–0.55 in Co(5–65)973, although the ratio was 1.2 for Co(90)973. The N/Co ratio of Co(5)973 was 5 but decreased with the cobalt content and reached the ratio of 0.3 for Co(65)973. The nitrogen atoms of cobalt molybdenum nitride in Co(35–65)973 were most likely bonded to molybdenum atoms rather than to the cobalt atoms.

On the other hand, the formation of MoO<sub>2</sub> was observed for Co(25)973 by XRD analysis as mentioned before (Figure 3). Since Co(50)973 contained a large amount of Co<sub>3</sub>Mo<sub>3</sub>N, the composition of cobalt molybdenum nitride was Co:Mo:N = 3:3:1.2 (≠2.3:2.3:1 from the XPS data; 2.5:2.5:1.0 from the elemental analysis). Since the Co/Mo ratio of cobalt molybdenum nitride in Co(50)973 was also 1.0 from the EDS analysis, the composition of cobalt molybdenum nitride was Co<sub>3</sub>Mo<sub>3</sub>N<sub>1.2</sub>. Cobalt molybdenum nitride in the bulk sample had a composition similar to Co<sub>3</sub>Mo<sub>3</sub>N obtained by Kim et al.<sup>22</sup> and Jackson et al.<sup>25</sup> Also, Bem et al.<sup>31</sup> reported similar compositions of Fe<sub>3</sub>Mo<sub>3</sub>N and Ni<sub>3</sub>Mo<sub>3</sub>N simulated by the Rietveld analysis method of the XRD data. Fe<sub>3</sub>Mo<sub>3</sub>N was reported to consist of the octahedral structure of NMo<sub>6</sub>.<sup>25,31</sup> The variety of the oxidation

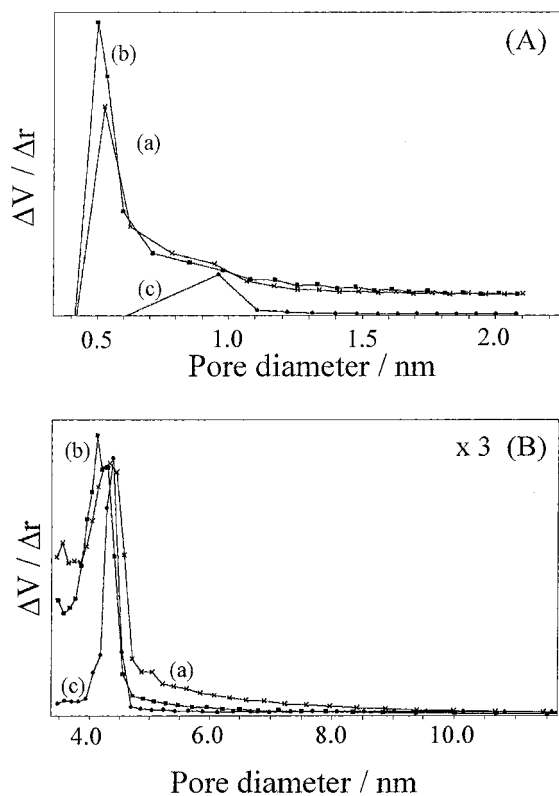


**Figure 6.** Pore size distribution of (A) mesopores and (B) micropores for the 973 K nitrated cobalt molybdenum: (a) Co(0)973; (b) Co(25)973; (c) Co(50)973.

states of Co and Mo can be explained by the coexistence of  $\text{Co}_3\text{Mo}_3\text{N}$ ,  $\gamma\text{-Mo}_2\text{N}$ , and Co metal (or Co nitride) from the XRD results in the Co(35–90)973 samples. Co(25)973 contained  $\text{MoO}_2$  and  $\gamma\text{-Mo}_2\text{N}$  (probably overlapped with Co–Mo oxynitride) in the XRD patterns (Figure 3). The presence of oxygen compounds such as  $\text{MoO}_2$  and Co–Mo oxynitride probably resulted in various Co and Mo oxidation states in the Co(5–25) samples. Another possibility is that the deconvolution of the Co and Mo spectra gave rise to some artifacts for obtaining a good curve fitting of the spectra of Mo  $3d_{5/2}$  and Mo  $3d_{3/2}$ .

**Surface Composition Measured by XPS.** The spectra of the XPS Mo 3d, Co 2p, and N 1s were deconvoluted in order to analyze the surface composition of the samples without argon etching in the XPS analysis. The distribution of Mo and Co ions on the surface of Co(0–100)973 is shown in Figure 10. The distribution of  $\text{Mo}^0$  and  $\text{Mo}^{2+}$  was about 30% for Co(20–65)973. The  $\text{Mo}^{3+}$ ,  $\text{Mo}^{4+}$ ,  $\text{Mo}^{5+}$ , and  $\text{Mo}^{6+}$  ions were less than 15% for the Co(5–65)973 sample, except for the Co(90)973 sample. The cobalt-rich samples contained a high abundance of  $\text{Mo}^{4+}$  and  $\text{Mo}^{5+}$ . The tendency of the Mo oxidation states on the surface was similar to those in the bulk of Co(35–65) samples. Furthermore, the distribution of  $\text{Co}^{2+}$  was more than 50% for all the samples, while  $\text{Co}^0$  and  $\text{Co}^{3+}$  were present in less than 40% amount. The distribution of  $\text{Co}^0$  was relatively low on the surface, compared to the bulk. The Co oxidation state on the surface became much higher than that in the bulk. The surface of Co(35–65)973 probably consisted of  $\text{Mo}^0$ ,  $\text{Mo}^{2+}$ , and  $\text{Co}^{2+}$  ions, which were the same species as in the bulk as already discussed. In Table 2, the surface composition of Co(0–35)973 had the N/Co ratio of greater than 7 while Co(50)973 was 1.1. The N/Mo ratio of the surface was 1.0 for Co(0–65)973 and 1.4 for Co(90)973. From the result, the surface nitrogen content of Co(50)973 was 2.5 times greater than that of  $\text{Co}_3\text{Mo}_3\text{N}$  in the bulk sample. The surface composition of

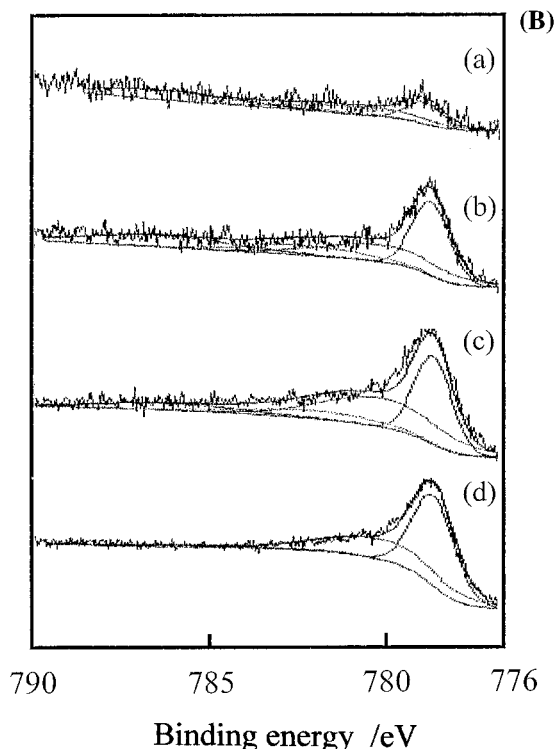
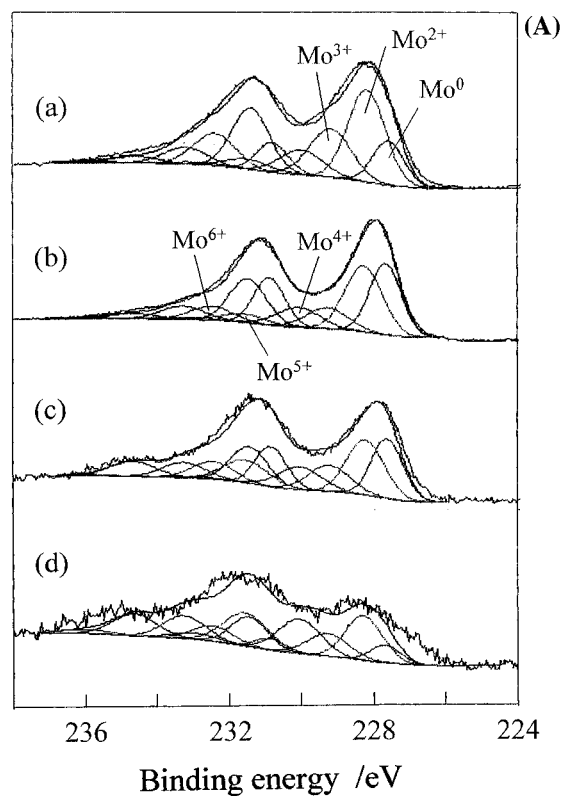


**Figure 7.** XPS spectra of (A) Mo 3d and (B) Co  $2p_{3/2}$  of bulk 973 K nitrated cobalt molybdenum. For (A): (a) Co(0)973; (b) Co(25)973; (c) Co(50)973; (d) Co(90)973. For (B): (a) Co(5)973; (b) Co(25)973; (c) Co(50)973; (d) Co(100)973.

Co(50)973 was  $\text{Co}_3\text{Mo}_3\text{N}_3$  ( $\text{Co}_3\text{Mo}_3\text{N}\cdot\text{N}_2$ ). From the results, the surface of the samples contained a number of nitrogens with molybdenum compared to the nitrogen content in the bulk.

**High Surface Area and Bulk Composition.** The relationship between the surface area and the bulk Mo 3d/Co 2p ratio is shown in Figure 11a, to determine the effect of the different

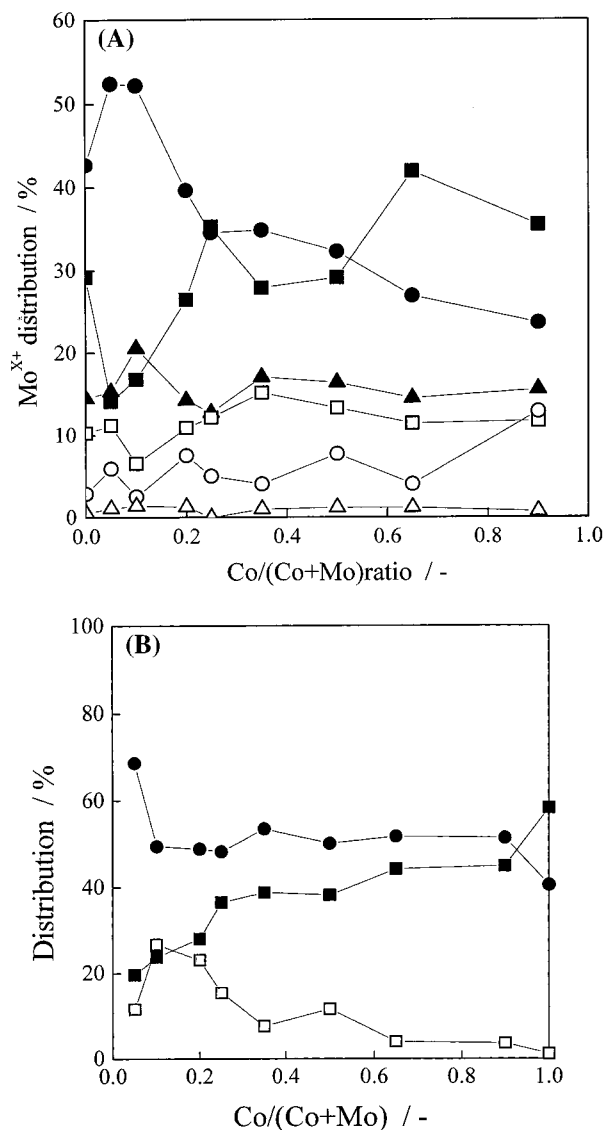


**Figure 8.** (A) Distribution of the Mo 3d spectra in the bulk as a function of Co/(Co + Mo) ratio for the 973 K nitrated cobalt molybdenum: (■) Mo<sup>0</sup>; (●) Mo<sup>2+</sup>; (▲) Mo<sup>3+</sup>; (□) Mo<sup>4+</sup>; (○) Mo<sup>5+</sup>; (△) Mo<sup>6+</sup>. (B) Distribution of the Co 2p spectra in the bulk as a function of Co/(Co + Mo) ratio for the 973 K nitrated cobalt molybdenum: (■) Co<sup>0</sup>; (●) Co<sup>2+</sup>; and (□) Co<sup>3+</sup>.

molybdenum ions in the bulk samples on the surface area. Since the surface area increased with the increasing Mo 3d/Co 2p ratio, the high surface area of the Co(10–25)973 samples was attributed to the Mo species in the bulk sample. However, the surface area was not related to the Mo 3d/Co 2p atomic ratio on the surface of the samples. In Figure 6, Co(0–25)973 had surface areas (120–129 m<sup>2</sup> g<sup>-1</sup>) that contained  $\gamma$ -Mo<sub>2</sub>N. The surface area of Co(50)973 was 12 m<sup>2</sup> g<sup>-1</sup> during the formation of Co<sub>3</sub>Mo<sub>3</sub>N, which was one-tenth the surface area of  $\gamma$ -Mo<sub>2</sub>N. Furthermore, Co<sub>3</sub>Mo<sub>3</sub>N in the Co(35–65)973 samples had mesopores without micropores at 0.4–0.6. In the relationship between the distribution of the surface area and the Mo<sup>2+</sup> ion in the bulk (Figure 11b), the surface area was proportional to the distribution of the Mo<sup>2+</sup> ion. However, the other Mo ions in the bulk and on the surface were not related to the BET surface area. The Co(5–25)973 samples mainly contained the Mo<sup>2+</sup> ion (about 50% in the distribution). Therefore, the surface area of the samples depended on the Mo<sup>2+</sup> ion in the bulk. Furthermore, the influence of the cobalt species in the bulk on these surface areas (Figure 11c) indicated that the surface area

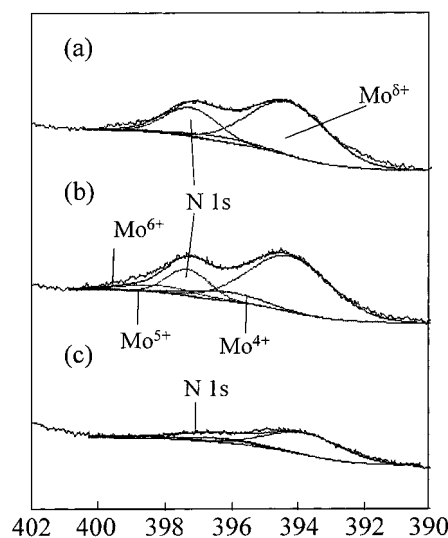


**Figure 9.** XPS spectra of N 1s and Mo 3p<sub>3/2</sub> in the bulk for the 973 K nitrated cobalt molybdenum: (a) Co(0)973; (b) Co(25)973; (c) Co(50)973; (d) Co(100)973.

**TABLE 1: Atomic Composition of Cobalt Molybdenum Nitride in Bulk with Various Co/(Co + Mo) Ratios**

sample	XPS/eV				composition <sup>b</sup>	elemental anal. composition <sup>c</sup>
	N 1s <sup>a</sup>	Co/Mo	N/Mo	N/Co		
Co(0)973	397.1	0	0.69		Mo <sub>1.4</sub> N	Mo <sub>1.2</sub> N
Co(5)973	396.8	0.10	0.50	5.12	Co <sub>0.2</sub> Mo <sub>1.4</sub> N	Co <sub>0.07</sub> Mo <sub>1.3</sub> N
Co(10)973	396.9	0.10	0.40	4.01	Co <sub>0.19</sub> Mo <sub>2</sub> N	Co <sub>0.2</sub> Mo <sub>1.4</sub> N
Co(20)973	396.8	0.10	0.37	3.41	Co <sub>0.28</sub> Mo <sub>2.7</sub> N	Co <sub>0.33</sub> Mo <sub>1.3</sub> N
Co(25)973	396.9	0.10	0.33	3.09	Co <sub>0.3</sub> Mo <sub>3</sub> N	Co <sub>0.42</sub> Mo <sub>1.25</sub> N
Co(35)973	396.2	0.31	0.54	1.77	Co <sub>0.59</sub> Mo <sub>1.9</sub> N	CoMo <sub>1.9</sub> N
Co(50)973	396.3	1.0	0.44	0.42	Co <sub>2.3</sub> Mo <sub>2.2</sub> N	Co <sub>2.5</sub> Mo <sub>2.5</sub> N
Co(65)973	396.3	1.4	0.39	0.26	Co <sub>3.6</sub> Mo <sub>2.5</sub> N	Co <sub>4.6</sub> Mo <sub>2.5</sub> N
Co(90)973	397.3	4.8	1.15	0.24	Co <sub>4.1</sub> Mo <sub>0.82</sub> N	nm <sup>d</sup>
Co(100)973	397.7			0.20	Co <sub>5</sub> N	Co <sub>20</sub> N

<sup>a</sup> Binding energies of N 1s. <sup>b</sup> Atomic composition obtained by XPS. <sup>c</sup> Atomic composition derived from the N/(Co,Mo) ratio obtained by elemental analysis. <sup>d</sup> Not measured.

was proportional to the content of Co<sup>3+</sup> ion but not on those of Co<sup>2+</sup> and Co<sup>0</sup> in the bulk. No cobalt species on the surface were related to the surface area. From these results, the insertion of Co<sup>3+</sup> ion into the bulk increases the distribution of Mo<sup>2+</sup> ion in the bulk which led to the increase in the surface area of the samples.

**Activity of Cobalt Molybdenum Nitrides for Thiophene HDS.** The rates of thiophene HDS on the various samples at 623 K with time on stream are shown in Figure 12. The Co(25)973 sample was the most active, but the Co(100)973 was the least. The HDS rate of the low Co-containing nitride samples (Co/(Co + Mo) = 0–0.35) reached a steady state after 1 h on stream, but the rates were kept constant for the high Co-containing samples (Co/(Co + Mo) = 0.5–1.0). The low Co-containing samples had higher activity than the high Co-containing samples on the basis of catalyst weight. The Co(25) sulfide catalyst was less active than the Co(0–25)973 catalysts. Concerning the HDS rate on surface area basis, the Co(35,50)-973 catalysts had a considerably higher HDS rate than the other catalysts at the initial stage and were more stable during the reaction. Since the sulfided catalyst had very low surface area, the sulfided Co–Mo catalyst exhibited higher HDS activity than the nitrated Co–Mo catalysts on surface area basis. Table 3 summarized the amount of irreversible CO adsorption and the catalytic data of the cobalt molybdenum nitride samples in

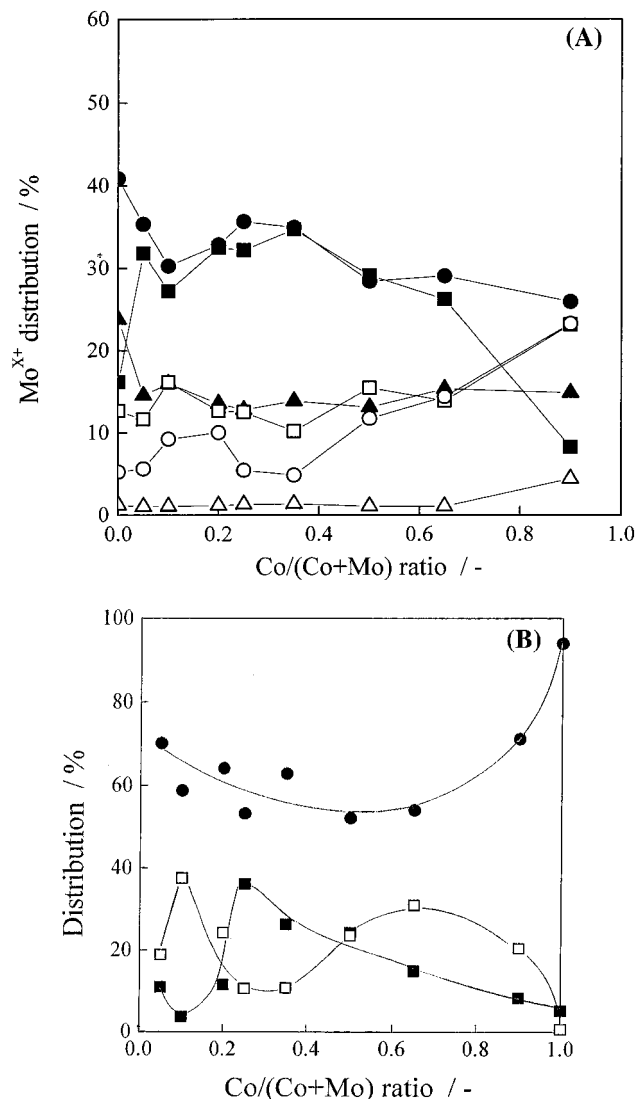


**Figure 10.** (A) Distribution of the surface Mo 3d spectra as a function of Co/(Co + Mo) ratio for the 973 K nitrated cobalt molybdenum: (■) Mo<sup>0</sup>; (●) Mo<sup>2+</sup>; (▲) Mo<sup>3+</sup>; (□) Mo<sup>4+</sup>; (○) Mo<sup>5+</sup>; (△) Mo<sup>6+</sup>. (B) Distribution of the surface Co 2p spectra as a function of Co/(Co + Mo) ratio for the 973 K nitrated cobalt molybdenum: (■) Co<sup>0</sup>; (●) Co<sup>2+</sup>; (□) Co<sup>3+</sup>.

**TABLE 2: Atomic Composition of Cobalt Molybdenum Nitride on the Surface with Various Co/(Co + Mo) Ratios by XPS**

sample	Co/Mo	N/Co	N/Mo	composition
Co(0)973	0		0.92	Mo <sub>1.1</sub> N
Co(5)973	0.05	18.7	1.00	Co <sub>0.04</sub> MoN
Co(10)973	0.08	11.9	0.95	Co <sub>0.08</sub> Mo <sub>1.1</sub> N
Co(20)973	0.10	6.75	0.93	Co <sub>0.16</sub> MoN
Co(25)973	0.10	11.3	1.04	Co <sub>0.08</sub> Mo <sub>0.96</sub> N
Co(35)973	0.11	8.7	1.00	Co <sub>0.13</sub> MoN
Co(50)973	0.97	1.05	1.02	Co <sub>0.95</sub> Mo <sub>0.98</sub> N
Co(65)973	1.37	0.68	1.01	Co <sub>1.4</sub> MoN
Co(90)973	3.58	0.39	1.4	Co <sub>2.7</sub> Mo <sub>0.7</sub> N
Co(100)973		0.35		Co <sub>2.9</sub> N

thiophene HDS. The low Co-containing samples exhibited high surface area and large amounts of CO adsorption. The amount of CO adsorption decreased with increasing Co content from Co(0) to Co(65)973 and then was present constantly in only a small amount. The samples of higher site densities for CO adsorption were Co(0,5)973 with high Mo content and Co(35,50)973 with Co<sub>3</sub>Mo<sub>3</sub>N. The TOFs of the low Co-containing samples (Co(5–50)973) exhibited two times or higher TOF than

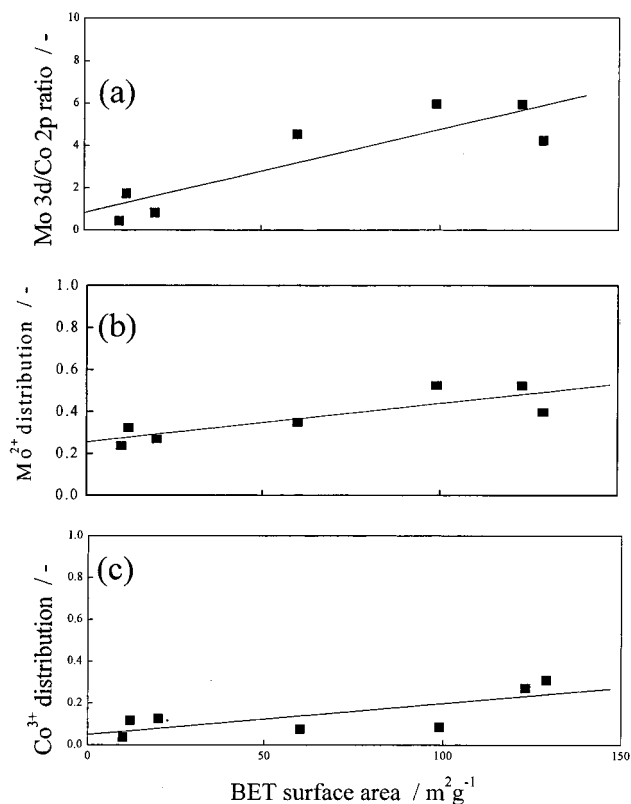


**Figure 11.** Relationship between the BET surface area and (a) bulk Mo 3d/Co 2p ratio, (b) the distribution of Mo<sup>2+</sup> and Mo<sup>3+</sup> in bulk, and (c) the distribution of Co<sup>3+</sup> in bulk.

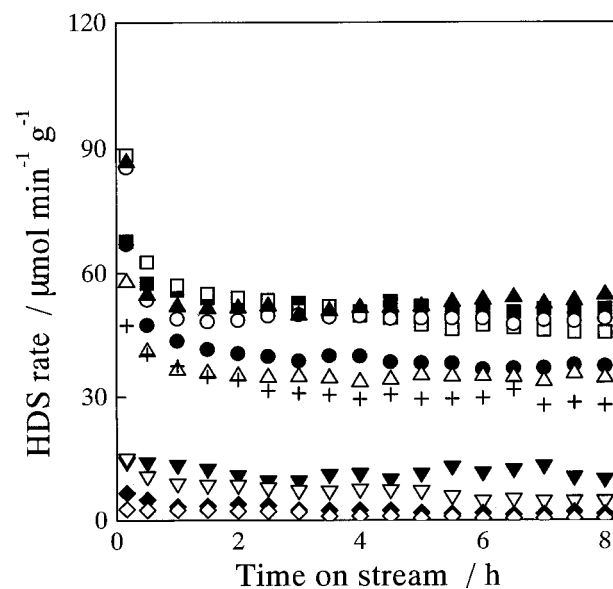


**Figure 12.** HDS of thiophene on various cobalt molybdenum nitrides with time on stream at 623 K: (■) Co(0)973; (□) Co(5)973; (●) Co(10)973; (○) Co(20)973; (▲) Co(25)973; (△) Co(35)973; (▼) Co(50)973; (▽) Co(65)973; (◆) Co(90)973; (◇) Co(100)973; (+) Co(25).

$\gamma$ -Mo<sub>2</sub>N (Co(0)973). Co<sub>3</sub>Mo<sub>3</sub>N was mainly formed in the Co(35,50)973 samples, although Co(65–100)973 exhibited ambiguous TOFs due to very small CO adsorption. Therefore, the formation of Co<sub>3</sub>Mo<sub>3</sub>N enhanced the activity of the catalysts for thiophene HDS. Kim et al.<sup>22</sup> reported that the HDS activity of Co<sub>3</sub>Mo<sub>3</sub>N was 4 times higher than that of  $\gamma$ -Mo<sub>2</sub>N on a surface area basis. Bussell and co-workers<sup>27</sup> also reported that the HDS activity of nitrated 6.7 wt % Co–12.8 wt % Mo/Al<sub>2</sub>O<sub>3</sub> (Co/Co + (Mo) = 0.48) catalysts was 4 times higher than that

**TABLE 3: Thiophene HDS Activity for Cobalt Molybdenum Nitrides**

sample	CO uptake <sup>a</sup> / $\mu\text{mol g}^{-1}$	HDS rate/ $\mu\text{mol min}^{-1} \text{m}^{-2}$ (BET surface area/ $\text{m}^2 \text{g}^{-1}$ )		TOF <sup>d</sup> / $\text{min}^{-1}$	C4 product distribn <sup>e</sup> /%				C4 selectivity <sup>e</sup>	
		initial <sup>b</sup>	steady <sup>c</sup>		<i>n</i> -butane	1-butene	<i>cis</i> -2-butene	<i>trans</i> -2-butene	<i>n</i> -butane 2-butenes	1-butene/ <i>trans</i> -2-butene
Co(0)973	372	0.60 (112)	0.68 (74)	0.19	60.4	9.8	13.0	16.8	2.03	0.58
Co(5)973	279	0.89 (99)	0.75 (61)	0.32	57.3	10.5	13.6	18.5	1.79	0.57
Co(10)973	207	0.54 (123)	0.69 (54)	0.32	54.7	10.1	14.8	20.4	1.55	0.495
Co(20)973	200	0.66 (129)	1.94 (25)	0.43	53.3	11.6	15.3	19.8	1.52	0.586
Co(25)973	166	0.70 (124)	1.19 (45)	0.54	54.1	11.3	14.6	20.0	1.56	0.565
Co(35)973	136	0.96 (60)	0.99 (35)	0.42	46.7	13.7	16.8	22.8	1.18	0.601
Co(50)973	21	1.19 (12)	1.12 (11)	0.68	37.2	17.2	18.7	26.9	0.82	0.639
Co(65)973	4.0	0.75 (20)	0.43 (11)	3.76	25.8	20.1	22.7	31.4	0.48	0.640
Co(90)973	5.8	0.66 (10)	0.17 (4)	1.14	18.4	26.3	23.3	32.0	0.33	0.822
Co(100)973	7.6	0.69(4)	0.11 (1)	0.35	nd <sup>e</sup>	nd <sup>e</sup>	nd <sup>e</sup>	nd <sup>e</sup>		
Co(25) <sup>f</sup>	25	15.8 (10)	21.6 (2)	1.88	39.3	15.0	26.2	19.5	0.65	0.769

<sup>a</sup> Irreversible CO adsorption. <sup>b</sup> After 10 min on stream. <sup>c</sup> After 8 h on stream. <sup>d</sup> TOF ( $\text{min}^{-1}$ ) = initial HDS rate ( $\mu\text{mol min}^{-1} \text{m}^{-2}$ )  $\times$  BET surface area ( $\text{m}^2 \text{g}^{-1}$ )/CO uptake ( $\mu\text{mol g}^{-1}$ ). <sup>e</sup> Not detected. <sup>f</sup> Sulfided at 623 K for 3 h under a stream of 10%  $\text{H}_2\text{S}/\text{H}_2$ .

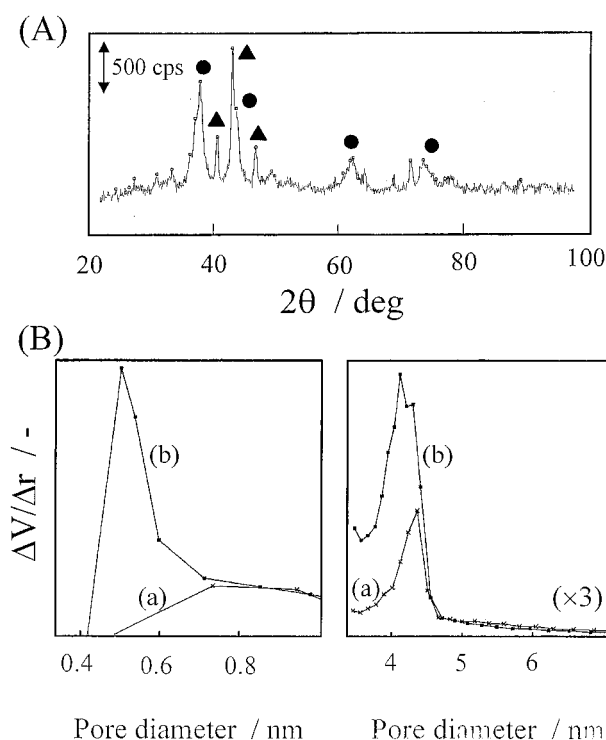


**Figure 13.** (A) XRD patterns after the reaction. (B) Pore size distribution of mesopores and micropores for Co(25)973: (a) after the reaction; (b) before the reaction.

of  $\gamma\text{-Mo}_2\text{N}/\text{Al}_2\text{O}_3$  on a  $\text{O}_2$  adsorption basis and found that the incorporation of Co species in the  $\text{Mo}_2\text{N}$  catalyst enhanced HDS activity of the nitrated Co–Mo/ $\text{Al}_2\text{O}_3$  catalyst.

The decrease in the BET surface area before and after the reaction was observed in Table 3. The surface area of the Co(0–35)973 samples extremely decreased after the reaction. The surface area of the Co(25)973 sample decreased from 124 to 45  $\text{m}^2 \text{g}^{-1}$  (36% decrease) after the reaction. Especially, the low-Co-containing samples exhibited great decrease in the surface area after the reaction. However, the surface area of Co(50)973 was unchanged before and after the reaction, indicating that  $\text{Co}_3\text{Mo}_3\text{N}$  was very stable. Although  $\text{Co}_3\text{Mo}_3\text{N}$  was not observed in Co(25)973 before the reaction (Figure 3b),  $\text{Co}_3\text{Mo}_3\text{N}$  was formed after the HDS reaction (Figure 13A). The increase in the activity of Co(25)973 on surface area basis (from 0.70 to 1.19  $\mu\text{mol min}^{-1} \text{m}^{-2}$ ) is probably due to the formation of  $\text{Co}_3\text{Mo}_3\text{N}$  during the reaction. Moreover, the (left) micropores and (right) mesopores for Co(25)973 in Figure 13B were formed largely before the reaction but decreased after the reaction. Since

$\text{Co}_3\text{Mo}_3\text{N}$  had small micropores, some remaining cobalts were crystallized with  $\gamma\text{-Mo}_2\text{N}$  in the presence of hydrogen to form  $\text{Co}_3\text{Mo}_3\text{N}$  in the bulk and led to the decrease in the surface area.

The reaction products were *n*-butane, 1-butene, *cis*-2-butene, and *trans*-2-butene with a very small amount of tetrahydrothiophene in thiophene HDS, as shown in Table 3. The distribution of *n*-butane formation was 60% for Co(0)973 with  $\gamma\text{-Mo}_2\text{N}$ , 54% for Co(10–25)973, and not more than 50% for Co(35–65)973 with  $\text{Co}_3\text{Mo}_3\text{N}$ . The hydrogenation selectivity (butane/2-butene ratio) of  $\text{Co}_3\text{Mo}_3\text{N}$  was 2 times lower than that of  $\gamma\text{-Mo}_2\text{N}$  and the sulfided catalyst. For the isomerization selectivity, 1-butene to *trans*-2-butene for all the samples slightly differed from a thermal equilibrium value (0.46). From the results,  $\text{Co}_3\text{Mo}_3\text{N}$  greatly desulfurized thiophene with lower hydrogen consumption than  $\gamma\text{-Mo}_2\text{N}$ . Therefore, cobalt molybdenum nitrides promise to be highly active catalysts for hydroprocessing of fuel oils and are more active than cobalt molybdenum sulfide on a catalyst weight basis.

## Conclusions

Cobalt molybdenum nitride was formed by the nitrating of  $\text{CoMoO}_4$  as a precursor via formation of Co–Mo oxynitride, while was not formed by the nitrating of CoO and  $\text{MoO}_3$ . The structure of the nitride samples depended on the oxidic precursors; that is,  $\gamma\text{-Mo}_2\text{N}$  was formed from  $\text{MoO}_3$  in Co(0–25)723,  $\text{Co}_3\text{Mo}_3\text{N}$  from  $\text{CoMoO}_4$  in Co(35–65)723, and Co metal and nitrides from CoO in Co(90–100)723. The TEM images showed that Co(50)973 consisted of several phases ( $\gamma\text{-Mo}_2\text{N}$  and  $\text{Co}_3\text{Mo}_3\text{N}$ ).  $\text{Co}_3\text{Mo}_3\text{N}$  contained predominantly cobalt and molybdenum species. The BET surface area was related to the bulk Mo 3d/Co 2p ratio, and furthermore, cobalt species penetrated into the bulk and increased the surface area of  $\gamma\text{-Mo}_2\text{N}$  for the low cobalt contents ( $\text{Co}/(\text{Co} + \text{Mo}) = 0.1–0.25$ ). The cobalt molybdenum nitrides were more active and selective than cobalt molybdenum sulfide on a catalyst weight basis for the HDS of thiophene with low hydrogenation selectivity.

**Acknowledgment.** We are grateful to Mr. T. Watabe and Ms. Y. Kondo (JEOL HIGH TECH, JEOL, Co., Ltd., Tokyo, Japan) for TEM analysis.

## References and Notes

- Markel, E. J.; Van Zee, J. W. *J. Catal.* **1990**, *126*, 643.
- Ozkan, U. S.; Zhang, L.; Clark, P. A. *J. Catal.* **1997**, *172*, 294.
- Nagai, M.; Miyao, T.; Tuboi, T. *Catal. Lett.* **1993**, *18*, 9.
- Nagai, M.; Takada, J.; Omi, S. *J. Phys. Chem. B* **1999**, *103*, 10180.

- (5) Nagai, M.; Irisawa, A.; Omi, S. *J. Phys. Chem. B* **1998**, *102*, 7619.
- (6) Park, H. K.; Lee, J. K.; Yoo, J. K.; Ko, E. S.; Kim, D. S.; Kim, K. L. *Appl. Catal. A.; Gen.* **1997**, *150*, 21.
- (7) Aegerter, P. A.; Quigley, W. W. C.; Simpson, G. J.; Ziegler, D. D.; Logan, J. W.; McCrea, K. R.; Glaizier, S.; Bussell, M. E. *J. Catal.* **1996**, *164*, 109.
- (8) Dolce, G. M.; Savage, P. E.; Thompson, L. T. *Energy Fuels* **1997**, *11*, 668.
- (9) McCrea, K. R.; Logan, J. W.; Tarbuck, T. L.; Heiser, J. L.; Bussell, M. E. *J. Catal.* **1997**, *171*, 255.
- (10) Nagai, M.; Goto, Y.; Ishii, H.; Omi, S. *Appl. Catal. A* **2000**, *192*, 182.
- (11) Zhang, Y.-J.; Xin, Q.; Ramos, I. R.; Ruiz, A. G. *Appl. Catal. A* **1999**, *180*, 237.
- (12) Markel, E. J.; Burdick, S. E.; Leaphart, M. E.; Roberts, K. L. *J. Catal.* **1999**, *182*, 136.
- (13) Schlatter, J. C.; Oyama, S. T.; Metcalfe, J. E.; Lambert, J. M. *Ind. Eng. Chem. Res.* **1988**, *27*, 1648.
- (14) Nagai, M.; Miyao, T. *Catal. Lett.* **1992**, *15*, 105.
- (15) Choi, J.-G.; Brenner, J. R.; Colling, C. W.; Demczyk, B. G.; Dunning, J. L.; Thompson, L. T. *Catal. Today* **1992**, *15*, 201.
- (16) Nagai, M.; Miyata, A.; Kusagaya, T.; Omi, S. In *The Chemistry of Transition metal Carbides and Nitrides*; Oyama, S. T., Ed.; Blackie: London, 1996; p 327.
- (17) Nagai, M.; Goto, Y.; Miyata, A.; Kiyoshi, M.; Hada, K.; Oshikawa, K.; Omi, S. *J. Catal.* **1999**, *182*, 292.
- (18) Lee, K. S.; Abe, H.; Reimer, J. A.; Bell, A. T. *J. Catal.* **1993**, *139*, 34.
- (19) Colling, C. W.; Thompson, L. T. *J. Catal.* **1994**, *146*, 193.
- (20) Sajokowski, D. J.; Oyama, S. T. *Appl. Catal. A.; Gen.* **1996**, *134*, 339.
- (21) Li, S.; Lee, J. S.; Hyeon, T.; Suslick, K. S. *Appl. Catal. A* **1999**, *184*, 1.
- (22) Kim, D.-W.; Lee, D.-K.; Ihm, S.-K. *Catal. Lett.* **1997**, *43*, 91.
- (23) Yu, C. C.; Ramanathan, S.; Oyama, S. T. *J. Catal.* **1998**, *173*, 1.
- (24) Ramanathan, S.; Yu, C. C.; Oyama, S. T. *J. Catal.* **1998**, *173*, 10.
- (25) Jackson, S. K.; Layland, R. C.; zur Loye, H.-C. *J. Alloys Compd.* **1999**, *291*, 94.
- (26) Li, Y.; Zhang, Y.; Raval, R.; Li, C.; Zhai, R.; Xin, Q. *Catal. Lett.* **1997**, *48*, 239.
- (27) Logan, J. W.; Heiser, J. L.; McCrea, K. R.; Gates, B. D.; Bussell, M. E. *Catal. Lett.* **1998**, *56*, 165.
- (28) Kojima, R.; Aika, K. *Chem. Lett.* **2000**, 514.
- (29) Ihm, S.-K.; Kim, D.-W.; Lee, D.-K. In *Catalyst Deactivation*; Bartholomew, C. H., Fuentes, G. A., Eds.; Elsevier Science: New York, 1997; p 343.
- (30) Jacobsen, C. J. H. *Chem. Commun.* **2000**, 1057.
- (31) Bem, D. S.; Gibson, C. P.; Loye, H.-C. *Chem. Mater.* **1993**, *5*, 397.
- (32) Chu, Y.; Wei, Z.; Yang, S.; Li, C.; Xin, Q.; Min, E. *Appl. Catal. A* **1999**, *176*, 17.
- (33) Yu, C. C.; Ramanathan, S.; Sherif, F.; Oyama, S. T. *J. Phys. Chem.* **1994**, *98*, 13038.
- (34) Quincy, B. R.; Houalla, M.; Proctor, A.; Hercules, D. M. *J. Phys. Chem.* **1990**, *94*, 1520.
- (35) Hada, K.; Nagai, M.; Omi, S. *J. Phys. Chem. B* **2000**, *104*, 2090.
- (36) Pawelec, B.; Navarro, R.; Fierro, J. L. G.; Vasudevan, P. T. *Appl. Catal. A* **1998**, *168*, 205.
- (37) Figueiredo, R. T.; Granados, M. L.; Fierro, J. L. G.; Vigas, L.; Piscina, P. R.; Homs, N. *Appl. Catal. A* **1998**, *170*, 145.
- (38) Zsoldos, Z.; Garin, F.; Hiaire, L.; Gucci, L. *Catal. Lett.* **1995**, *33*, 39.
- (39) Nagai, M.; Omata, T.; Omi, S. Manuscript in preparation.
- (40) Nagai, M.; Koizumi, K.; Omi, S. *Catal. Today* **1997**, *35*, 393.
- (41) Hada, K.; Nagai, M.; Omi, S. Manuscript in preparation.
- (42) Gucci, L.; Sundararajan, R.; Koppány, Zs.; Zsoldos, Z.; Schay, Z.; Mizukami, F.; Niwa, S. *J. Catal.* **1997**, *167*, 482.
- (43) Okamoto, Y.; Nakano, H.; Imanaka, T.; Teranishi, S. *Bull. Chem. Soc. Jpn.* **1975**, *48*, 1163.
- (44) Fix, R.; Gordon, R. G.; Hoffman, D. M. *Thin Solid Films* **1996**, *288*, 116.
- (45) Nakajima, T.; Shirasaki, T. *J. Electrochem. Soc.* **1997**, *144*, 2096.
- (46) Milad, I. K.; Smith, K. J.; Philip C. W.; Mitchell, A. R., *Catal. Lett.* **1998**, *52*, 113.